Vol. 5 No. 1 (2026)

Pakistan Journal of Medical & Cardiological Review

https://pakjmcr.com/index.php/1/about

Online ISSN 3007-2387

Print ISSN 3007-2379

MEBEVERINE-LOADED ISPAGHOL PSYLLIUM HYDROGEL: ADVANCING TREATMENT STRATEGIES FOR IBS

Anam Tariq
Department of Pharmaceutics, Faculty of Pharmacy, Superior University, Lahore, Pakistan.
anamtariqpharmacist@gmail.com
Syed Muhammad Aun
Department of Pharmaceutics, Faculty of Pharmacy, Superior University, Lahore, Pakistan
Hashir Shehbaz
Faculty of Pharmacy, University of Lahore, Lahore, Pakistan
Ghanwa Tariq
Department of Pharmaceutics, Faculty of Pharmacy, Superior University, Lahore, Pakistan
Ahmad Hussain Anjum
Department of Pharmaceutics, Faculty of Pharmacy, Superior University, Lahore, Pakistan

Author Details

Keywords:

Received: 14 December 2025
Accepted: 29 January 2026
Published: 13 February 2026

Corresponding E-mails & Authors*:
Anam Tariq
anamtariqpharmacist@gmail.com

Abstract

This study developed novel pH-responsive interpenetrating network (IPN) hydrogels from ispaghula psyllium gel (IPG), PEG 6000, methacrylic acid (MAA), and N,N'-methylene bisacrylamide (MBA) for sustained oral delivery of mebeverine HCl (MBV) to treat irritable bowel syndrome (IBS). IPG was extracted via modified water method, and nine formulations (PsPM1–9) were synthesized by free-radical polymerization, varying component ratios.

MBV loading reached 61–86% via swelling-diffusion, with gel fractions of 86–96%. FTIR, DSC, TGA, and SEM confirmed compatibility, thermal stability (degradation >460 °C), and porous morphology ideal for swelling (up to 97% at pH 7.4 vs. <13% at pH 1.2).

In vitro release at pH 7.4 (up to 89% over 24–36 h) was higher than at pH 1.2, tuned by components: IPG/PEG/MAA enhanced it via hydrophilicity/repulsion, while MBA reduced it by densification. Zero-order and Korsmeyer-Peppas models best fit (R^2 0.91–0.98), with super Case II transport (n 0.93–1.52).

These biocompatible hydrogels offer promise for colon-targeted MBV delivery, reducing dosing frequency and improving IBS patient compliance.

INTRODUCTION

Hydrogel formulations are primarily composed of various polymers, monomers, initiators, and cross-linkers. When these components are mixed, they have a significant effect on the swelling behavior of hydrogel. Most of the hydrogel system uses are dependent on the polymeric network's swelling pattern. Changing formulation components has a direct impact on hydrogel swelling behavior, which in turn influences drug release behavior (Hazer et al., 2008).

Polymers are lengthy chains of macromolecules to which various functional groups are bonded. The pharmaceutical and food industries use polymers of both natural and synthetic origin (Singh et al., 2011). Natural and synthetic polymers are equally accessible, but natural polymers are preferred owing to their benefits over synthetic polymers. Naturally occurring polymers are inexpensive, widely accessible, inert, non-toxic, biocompatible, and biodegradable (Bahadur et al., 2017).

Ispaghol belongs to the PLANTAGO plant family, and its seeds are used to produce mucilage. Husk is primarily used as a dietary fibre; it contains both soluble and insoluble fibre as well as natural laxatives, making it an efficient cure for constipation. When consumed, it causes the stomach to expand and aids in the removal of the contents. Because of its hygroscopic properties, it absorbs water from the gastrointestinal tract, improving stool consistency and so reducing constipation. When consumed, husk develops a protective barrier around the stomach, protects against corrosion, and provides relief from acidity.

Polyethylene glycol (PEG) is a preferred polymer in drug delivery systems. When choosing an excipient for formulation development, this polymer's adjustable characteristics and known safety profile are crucial factors that contribute to its popularity. PEG is well-known for its high structural flexibility, hydrophilicity, biocompatibility, amphiphilicity, absence of steric barriers, and a substantial hydration potential. PEG 100 to PEG 700 are liquids at ambient temperature, while PEG 1000 to 2000 are soft substances.

The antispasmodic drug Mebeverine hydrochloride (HCl) has been used per orally in the symptomatic treatment of bowel disturbances and intestinal discomfort related to irritable bowel syndrome (Abdel-Hamid et al., 2007).

Mebeverine HCl is a musculotropic antispasmodic with no atropic side effects. Its primary therapeutic use is to treat IBS. It has a 75% plasma protein binding rate, a brief biological half-life of 2.5 hours, and rapid absorption from the upper gastrointestinal tract following oral intake, with highest plasma levels occurring in 1-3 hours. Mebeverine HCl was chosen as a model medicine because it had all the required pharmacokinetic and physicochemical features for controlled supply (El Nabarawi et al., 2017).

The present study was designed to incorporate Mebeverine HCl in a biodegradable IPN based on naturally existing Isabgol psyllium's gel and a synthetic substance PEG 6000 for controlled drug delivery which has been expected to lower the frequency of doses as well as improve patient compliance. To our knowledge oral delivery of Mebeverine HCl through hydrogels have not been studied to such an extent before.

1.1. Controlled drug delivery system (CDDS)

Controlled drug delivery keeps therapeutic levels steady at the target site, cutting toxicity, side effects, and dosing frequency while boosting bioavailability and avoiding under- or overdosing (Uhrich et al., 1999; Jethara & Patel, 2014). These systems—using biodegradable polymers, microparticles, liposomes, hydrogels, and more—respond to stimuli like pH or temperature for precise release (Bhagwat & Vaidhya, 2013; Fig. 1; Saikia & Gogoi, 2015).

Pakistan Journal of Medical & Cardiological Review
https://pakjmcr.com/index.php/1/about
Online ISSN 3007-2387
Print ISSN 3007-2379



Figure 1. Advantages of Controlled drug Delivery System

1.2. Isabgol husk

Isabgol husk, also known as psyllium husk, is a naturally occurring water-soluble polymer derived from the dried mature seeds of the Plantago ovata plant, which belongs to the Plantaginaceae family. The hydrophilic fibrous mucilage presents abundantly in seeds. Isabgol husk is commonly used as a traditional medicine for ailments such as constipation, diabetes, ulcers, and hyper-cholesterolaemia. Because of its swelling and gelling mass capabilities, it has sparked interest in pharmaceutical drug delivery systems to produce hydrophilic matrix and encapsulating microparticulate. An attempt was made to crosslink the husk with several synthetic polymers. Singh B. et al. modified husk with methacrylamide using 60Co gamma radiation crosslinked polymerization to manufacture a sustained release rifampicin hydrogel (Ale et al., 2023).

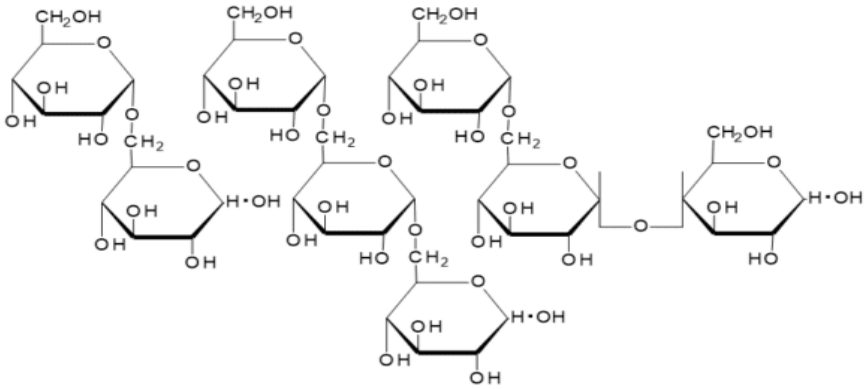

Figure 2. Structural formula of Isabgol psyllium husk (Arabinoxylan)

Chaplin et al.,2000 reported that Psyllium supplements may benefit the treatment of irritable bowel syndrome, inflammatory bowel disease, and ulcerative colitis. However, the therapy should persist for longer than a month, as no improvement was shown in another 30-day experiment. Although there is little evidence to support fiber's usefulness in treating simple diverticulitis, it has been routinely utilized by patients to alleviate overall discomfort (Chaplin et al.,2000).

1.3. Polyethylene Glycol 6000

Polyethylene glycol (PEG) is the preferred polymer for drug delivery technologies. This substance is valuable because of its adjustable capabilities and widely recognized safety record, both of which are important factors to consider when selecting an excipient for formulation development.

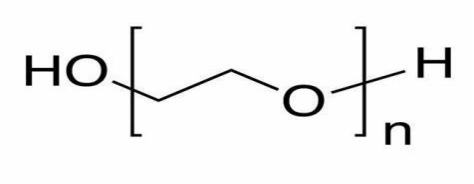

Figure 3. Structural formula of PEG 6000

2. Materials and methods

2.1 Extraction of gel from Ispaghul psyllium seeds

Arabinoxylan, the predominant hemicellulose in Ispaghul psyllium seeds (IPS), was recovered using a modified water extraction method (Ahmad et al., 2021). IPS (5% w/v) was dispersed in distilled water, stirred magnetically at 500 rpm for 1 h, and soaked for 24 h at 25 °C. The resulting gel was vacuum filtered through muslin cloth, air-dried to form gum layers, pulverized into fine powder (IPG), and stored in an airtight container for further use.

2.2. Synthesis of psyllium/PEG-co-MAA hydrogel

We prepared nine hydrogel formulations by mixing varying ratios of IPG, PEG 6000, MAA, and MBA. IPG was soaked and stirred (450 rpm) in distilled water until it was clear; PEG 6000 was similarly dissolved. The solutions were combined, then ammonium persulfate initiator, warmed MAA monomer, and pre-dissolved MBA crosslinker were added with stirring until homogeneous. The mixture was pipetted into sterile test tubes, degassed in a sonicator (50 °C, 3–5 min), foil-sealed, and polymerized in a water bath (Memmert, Japan) at 55 °C for 12 h. After cooling, hydrogels were extruded, sliced into discs, soaked in water:methanol (50:50 v/v; 15–20 min), dried (55–60 °C), and stored in zip bags for testing (Olad et al, 2018).

Table 1. Composition of psyllium/PEG network formulations

Code	Psyllium (g/30ml)	PEG 6000 (g/30ml)	MAA (g/30ml)	MBA (g/30ml)	APS (g/30ml)
PsPM1	0.3	0.15	6	0.06	1.2
PsPM2	0.6	0.15	6	0.06	1.2
PsPM3	0.9	0.15	6	0.06	1.2
PsPM4	0.6	0.3	6	0.06	1.2
PsPM5	0.6	0.6	6	0.06	1.2
PsPM6	0.6	0.3	7.5	0.06	1.2
PsPM7	0.6	0.3	9	0.06	1.2
PsPM8	0.6	0.3	6	0.12	1.2
PsPM9	0.6	0.3	6	0.18	1.2

2.3. Characterization

2.3.1. Loading of Mebeverine hydrochloride (MBV) into hydrogel discs

Precisely 1 g MBV powder was weighed into a dry 250 mL beaker, dissolved in phosphate buffer (final volume 100 mL) with stirring, and adjusted to ensure complete dissolution. Pre-weighed hydrogel discs were immersed in the MBV solution until swelling equilibrium. Swollen discs were removed, rinsed with water, surface-dried with filter paper, and oven-dried at 45–50 °C (Hussain et al., 2022). MBV loading (%) was calculated via the weight method using the following equation.

$$MBV\ loading\ (\%) = \left[\frac{w_d - w_0}{w_d}\right] \times 100$$

Where *Wo* and *Wd* represent the weight of carrier pre and post soaking in the drug solution, respectively.

2.3.2. Sol-gel fraction analysis

This study examined the psyllium/PEG-co-MAA hydrogel network to find out its reacted and unreacted constituents. Dried formulations' discs were weighed and transformed to small sized pieces by crushing. In order to expel the unreacted reactants from polymerized network, extraction process was carried out for four hours in Soxhelt apparatus having distilled water with boiling temperature. The extracted hydrogel's fragments were collected, dried at room temperature for 24 hours and then in a hot air oven set at 45 to 50°C before being reweighed. The following formulas were used to compute the sol-gel fraction (Liang et al, 2019).

$$Sol\ fraction\ (\%) = \left[\frac{w_0 - w_i}{w_0}\right] \times 100$$

$$Gel\ fraction\ (\%) = 100 - Sol\ fraction$$

Here, W_o and *Wi* were the weight of network disc before and after extraction procedure, respectively.

2.3.3. Fourier Transforms Infrared Spectroscopy

To verify the complex formation and components compatibility, FTIR analysis was performed on pure mebeverine, PEG, IPG, mixture of constituents, mebeverine-loaded and unloaded cross-linked

network. After mixing with KBr, all of the samples were dried and crushed. A 12-mm-thick disc was then created by applying 65 kN of pressure for one minute. These materials were scanned using an FTIR spectrophotometer (Thermos Fischer Scientific Nicolet 6700 TM) at 4000 to 500 cm^{-1} (Che et al, 2016).

2.3.4. Differential Scanning Calorimetry (DSC)

Differential Scanning Calorimetry (DSC) experiments were carried out to verify the created network's crystalline or amorphous nature as well as its phase transition behavior (melting temperature). This approach quantifies the absorbed and emitted energy in relation to the material's condition during heating or cooling phase.

A Q2000 series thermal analyzer (TA Instruments, West Sussex, Chichester, UK) was used to conduct the analysis. In practice, 1-3 mg of the sample was precisely weighed and sealed in an aluminum pan. DSC investigations were carried out using a heating rate of 20 ◦C/min and a temperature range of 25 ◦C to 400 ◦C. To keep the environment inert, 20 mL of nitrogen gas was added every minute (Hussain et al, 2021).

2.3.5. Thermogravimetric analysis (TGA)

This experiment was performed to document mass changes in relation to heat fluctuations. A TG/DTA apparatus from the Pyris Diamond series (Perkin Elmer, USA) was utilized to conduct the study. Briefly, accurately weighed samples were smashed and to assure the size consistency passed through sieve # 40. These samples with weight ranging within 0.08-8 mg were provided with a temperature of 40 degrees celsius for one minute. After then, the temperature was raised at a rate of 10 degrees Celsius per minute, beginning at 40 degrees Celsius and reaching 600 degrees Celsius while the environment remained inert. Each experiment was done in triplicate to assure the precision of findings (Suhail et al, 2021).

2.3.6. Scanning electron microscopy (SEM)

To investigate the surface structure of the created network, microscopy pictures were obtained at various resolutions. This study is used to display features including fractures, waviness, porosity, and smoothness on the surfaces. The hydrogel network's swelling and release characteristics are mostly assessed by surface morphology. SEM analyses were carried out following a 40-second sputter coating of a thin layer of gold over the samples' exposed surfaces, in a vacuum. The Hitachi S4800 scanning electron microscope was used for close inspection of the surface and to take pictures (Najafian et al, 2022).

2.3.7. *In-vitro* swelling experiments

The swelling capability of the psyllium/PEG-co-MAA system at both alkaline and acidic pH values was measured in order to evaluate its pH sensitivity. The dry hydrogel discs used in this experiment were weighed first and then submerged in buffer solutions with pH levels of 1.2, 6.8 and 7.4. At certain intervals of 0, 0.5, 1, 2, 4, 6, 10, 14, 20, 26, 32, 38, 46, 56, and 72 hours, the discs were taken out of their corresponding solutions and reweighed after being swabbed. The following formula was used to calculate the percentage equilibrium swelling at the conclusion of the experiment.

$$Equilibrium\ swelling = \frac{ws - w_d}{w_d} \times 100$$

Where Ws represented the weight of the swelled hydrogel at certain intervals, while Wd represented the beginning weight of the dry hydrogel.

2.3.8. *In vitro* Mebeverine release Experiments

To explore how formulation components and pH affect mebeverine release from psyllium/PEG hydrogels, we ran dissolution tests in buffers at pH 1.2, 6.0, and 7.4. Mebeverine-loaded discs were placed in basket holders of a USP Type II dissolution apparatus filled with 900 mL buffer, maintained at 37 ± 0.5 °C. At set intervals (0.5, 1, 1.5, 2, 3, 4, 5, 6, 9, 12, 15, 18, 24, 30, and 36 h), we withdrew 5 mL samples from the vessel's center, replacing them with fresh buffer to maintain

sink conditions. Samples were diluted, filtered, and analyzed for absorbance at λ_max 263 nm using a UV-Vis spectrophotometer (Shimadzu, Japan). Mebeverine concentrations were calculated from a standard curve's linear equation (Ravishankar et al., 2019).

2.3.9. Application of kinetic models on released data

Drug release from our hydrogels depends on factors like drug loading, polymer/monomer/crosslinker amounts, swelling behavior, and drug diffusion through the swollen matrix. To identify the best-fitting kinetic model and release mechanism, we analyzed data using zero-order, first-order, Higuchi, and Korsmeyer-Peppas models via the DD Solver Excel add-in. The highest regression coefficient (R^2) indicated the top match.

From the Korsmeyer-Peppas model, the release exponent "n" revealed the transport type: $n \leq 0.5$ signals Fickian diffusion; $0.5 < n < 1$ shows anomalous (non-Fickian) transport; and $n = 1$ indicates Case II relaxation.

The following kinetic models were used to analyze release data:

Zero order

$$Q_t = Q_0 - k_0 t$$

First order

$$log\ Q = log\ Q_0 - (k_1 t\ /\ 2 \cdot 303)$$

Higuchi model

$$Q_t = k_{ht}{}^{1}/_{2}$$

Hixen-Crowell model

$$Q_0^{1/3} - Q_t^{1/3} = -k_{HC} t$$

In above equations

Q_t is the proportion of mebeverine released from network after time, t, Q_o represents the initial quantity of mebeverine in hydrogel and Q accounts for the drug still to be released from the hydrogel. k_o, k_1, k_h and K_{HC} are zero order, first order, Higuchi and Hixen-Crowell rate constants, respectively.

Korsemeyer Peppas model

Pakistan Journal of Medical & Cardiological Review
https://pakjmcr.com/index.php/1/about
Online ISSN 3007-2387
Print ISSN 3007-2379

$$M_t / M_\infty = k_p t^n$$

Where M_t / M_∞ is the amount of drug released in time t and k_p is the power-law constant and n denotes release exponent.

3. Results and discussion

3.1. Appearance of Psyllium/PEG hydrogels

Formulated network as withdrawn from glass tubes, exhibited soft and flexible framework showing off-white color. Discs of hydrogel transformed to brown, amber in color upon drying. Slight alterations were observed in the texture on varying the IPG, PEG, MAA and MBA proportions. Figures 4 and 5 demonstrate the actual appearance of freshly produced and dried form of hydrogels.

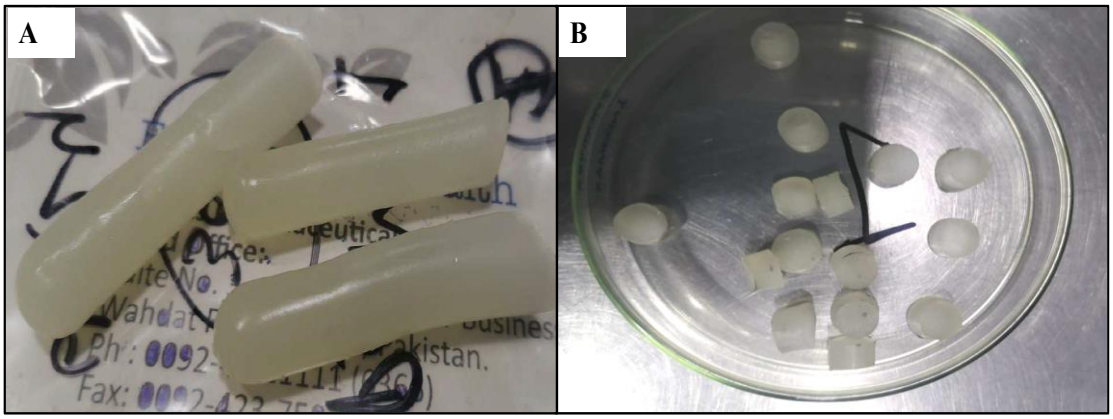

Figure 4. Psyllium/PEG hydrogel rods (A) and discs (B)

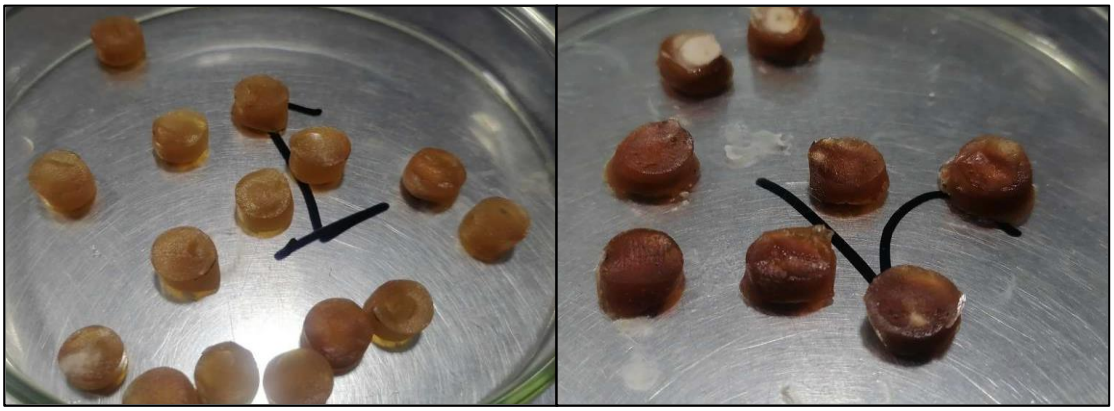

Figure 5 Dried form of psyllium/PEG hydrogel discs

3.2 Mebeverine loading

Psyllium/PEG-co-MAA hydrogels (PsPM1–9) were loaded with 1% w/v MBV via diffusion; loading efficiency varied with IPG, PEG, MAA, and MBA ratios due to swelling differences (Fig 5).Increasing IPG (0.3–0.9 g; PsPM1–3) raised loading from 61.08% to 69.72%; PEG (0.15–0.6 g; PsPM3–5) pushed it to 69.66–75.18%. Higher MAA (6–9 g; PsPM5–7) boosted it further to 85.98%, as anionic COO^- groups enhanced swelling via chain repulsion—mirroring Mahmood et al. (2019) on lovastatin at pH 7.4.

Conversely, more MBA (0.06–0.18 g; PsPM7–9) dropped loading to 72.26%, consistent with Malatani et al. (2023) on mucin-chitosan microparticles.

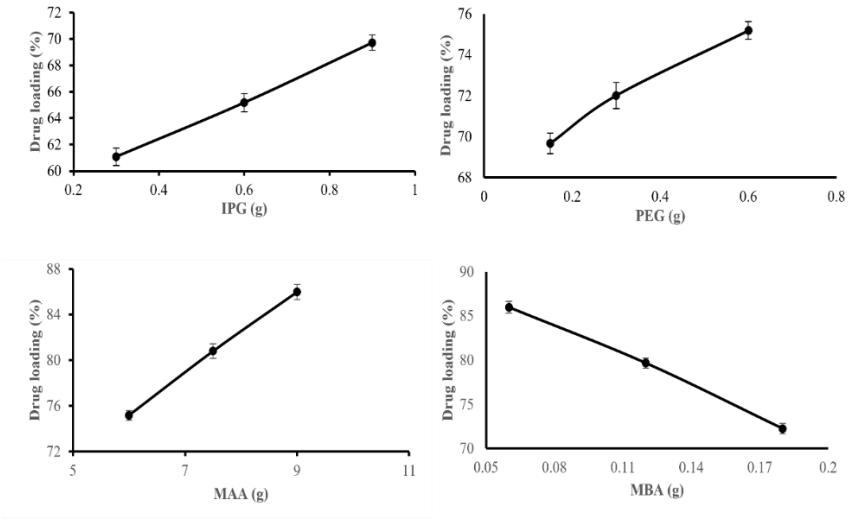

Figure 6. Impact of network components on MBV loading%

3.3 Sol-gel fraction determination

To see how IPG, PEG, MAA, and MBA affect sol/gel fractions, we tested all formulations (PsPM1–9), which showed gel fractions of 86.48–96.12% (Fig 6). Higher amounts of each component boosted gel content by tightening the network.

IPG/PEG increases (PsPM1–5) raised gel from 70.84% to 80.81%. More MAA (PsPM5–7) pushed it to 89.01%, strengthening hydrogen bonding and cutting sol fraction—matching Batool et al.

(2021). MBA addition (PsPM7–9) further increased gel to 95.10%, creating a denser structure, as seen in Sahraei and Ghaemy (2017).

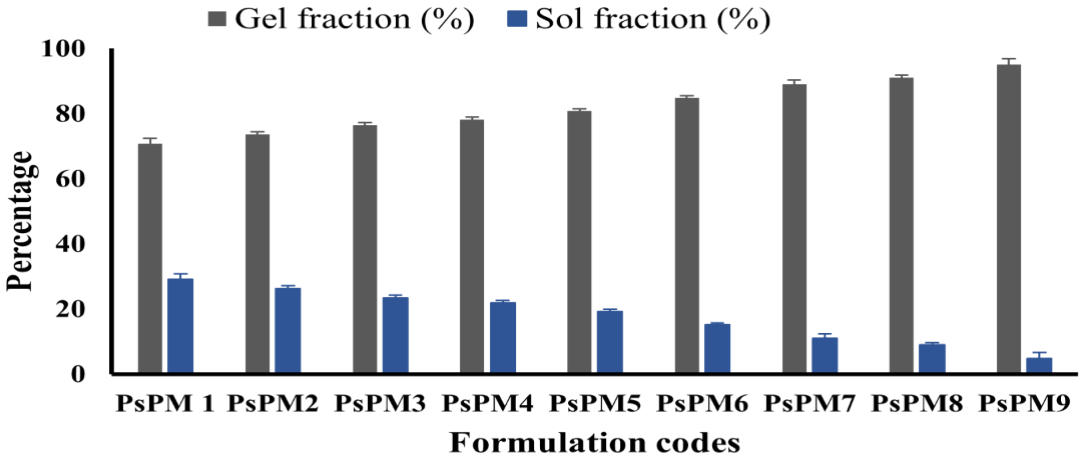

Figure 7. Gel and sol fraction of hydrogels (PsPM1-PsPM9)

3.4. FTIR examination

FTIR analysis of pure MBV, IPG, PEG, MAA, and the psyllium/PEG hydrogel confirmed compatibility and network formation (Fig. 4.5).

IPG showed a broad -OH stretch at 3311.97 cm^{-1}, C-O at 2920.41 cm^{-1}, C=O (galacturonic acid) at 1745.72 cm^{-1}, and C-O-C bands (1647.83–985.02 cm^{-1})—matching Singh et al. (2022) on psyllium hydrogels.

Pakistan Journal of Medical & Cardiological Review
https://pakjmcr.com/index.php/1/about
Online ISSN 3007-2387
Print ISSN 3007-2379

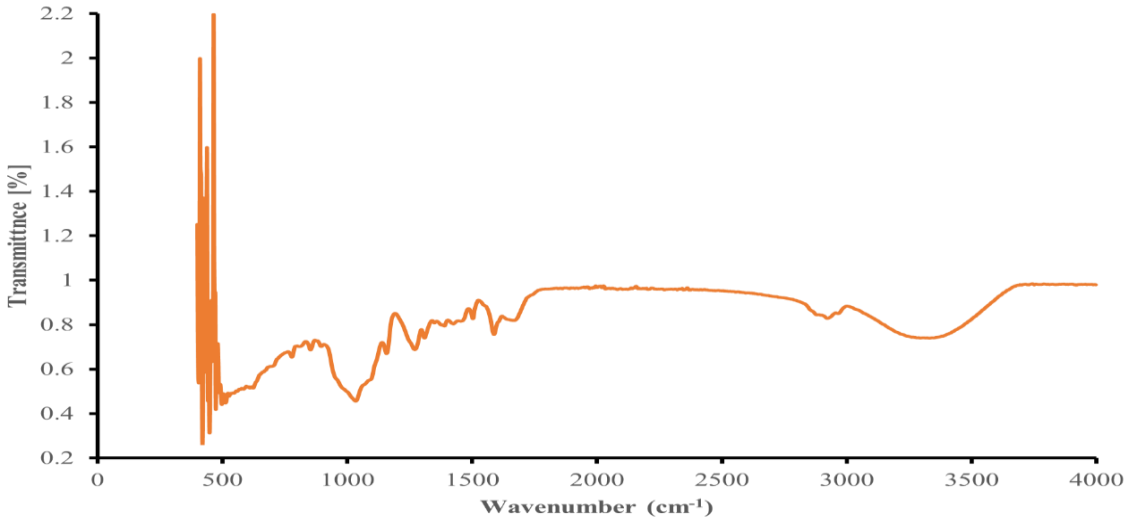

Figure 8. FTIR spectrum of ispaghul psyllium

The PEG spectrum presented clear transmittance peaks at 2875.54 cm^{-1}, 1323.56 cm^{-1} and1278.70 cm^{-1} signifying the alkyl units, C-H bending and C-H twisting movements, respectively. Whereas, stretching movements relating to carbonyl and ether groups were confirmed by evident bands at 1121.66 cm^{-1} and 1093.11 cm^{-1} on IR spectrum of polymer (Zahra et al, 2022). Spectrum of PEG is displayed in figure 8.

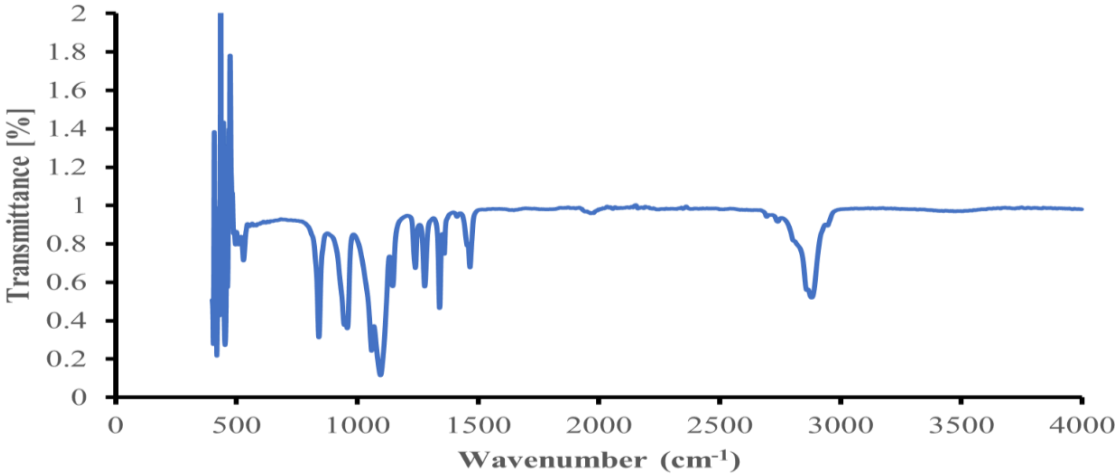

Figure 9. FTIR spectrum of PEG 6000

For Mebeverine HCl, movements due to C=O and C=C bonds were evident by existence of transmittance bands at 1605 cm^{-1} and 1519.34 cm^{-1} on IR spectrum. Another prominent feature was noticed at 1060.48 cm^{-1} demonstrating the C-N bond in Mebeverine structure (Almukhtar and Karam 2020). Spectrum is shown in figure 10.

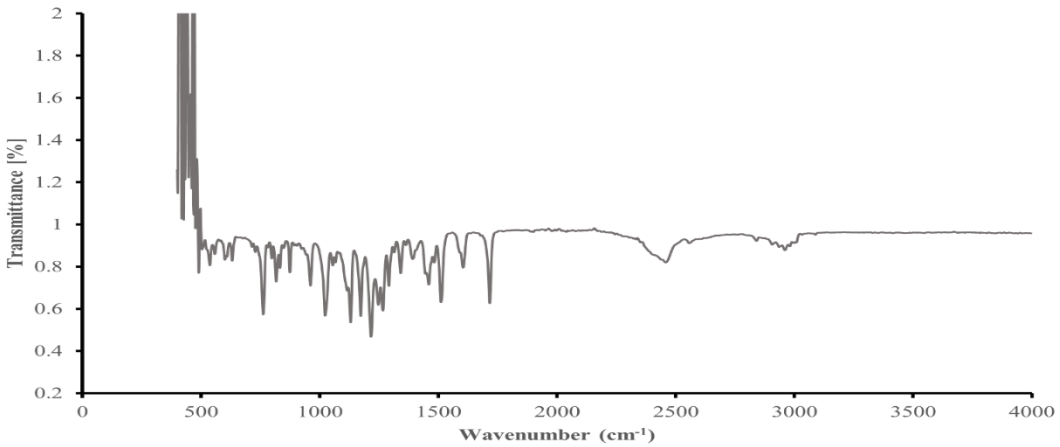

Figure 10. FTIR spectrum of Mebeverine HCl

On the IR spectrum of methacrylic acid, the occurrence of typical peaks was shown at 1711.05 cm^{-1} linked to C=O stretch movements of carboxylic unit and at 1688.61 cm^{-1} due to vinyl group unsaturation triggering C=C stretching. Moreover, some peaks at 1454.08 cm^{-1}–1199.16 cm^{-1} range on spectrum were indicating the C-O and C-H movements. As shown in our analysis, Rasib et al. (2017) also verified the comparable pattern of peaks on MAA spectrum. All these peaks can be seen on the IR spectrum shown in figure 11.

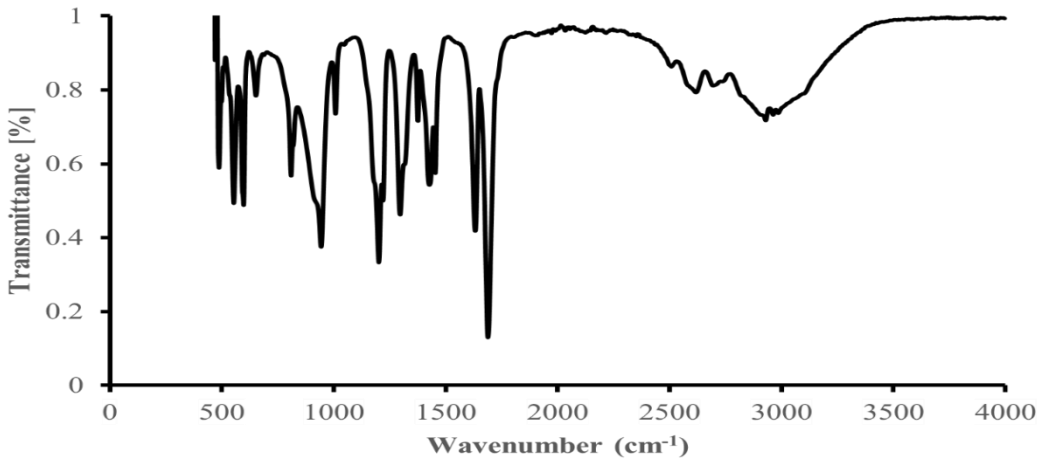

Figure 11. FTIR spectrum of MAA

Using FTIR analysis, the psyllium/PEG network was also investigated for different groups and showed the transition of several peaks of distinct components in the hydrogel network. On the IR spectra of unloaded hydrogels as seen in figure 12, a clear band clearly formed at 1271.58 cm^{-1} was the result of C--H twisting in PEG being relocated from the position of 1278.70 cm^{-1} on PEG's spectrum. Another visible feature of PEG at 1121.66 cm^{-1} relating to carbonyl groups was shifted towards slightly higher wavenumber of 1160.41 cm^{-1} on hydrogel's spectrum. The creation of the new grafted system was confirmed by these differences in peak locations and intensities.

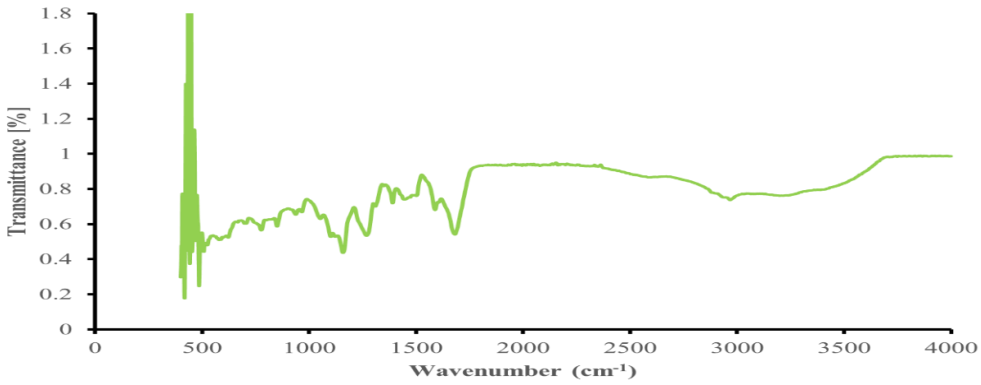

Figure 12. FTIR spectrum of unloaded psyllium/PEG hydrogel

The hydrogel network encapsulated with MBV, as seen in Figure 13, exhibited peaks of IPG, PEG, MAA and MBV with minor modifications, guaranteeing the grafting of components to create a complex system. The characteristic band of MBV due to C=O bond at 1605 cm^{-1} was displaced to 1696.77 cm^{-1} with slightly reduced intensity on the formulation's IR spectrum. Moreover, some specific peaks of PEG and IPG were also presented with slight shifting and modification of intensities. MBV loading inside the network was proven by the development of typical peaks of the drug on the IR spectra of psyllium/PEG-co-poly (MAA) hydrogels.

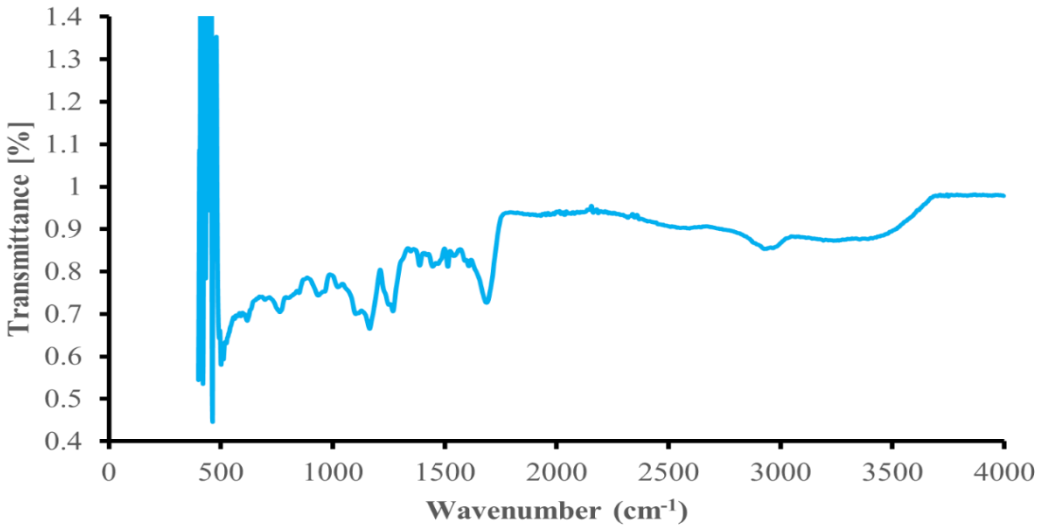

Figure 13. FTIR spectrum of MBV loaded hydrogel

3.5. Differential Scanning Calorimetry (DSC) and thermogravimetric analysis (TGA)

DSC and TGA assessed thermal properties of psyllium/PEG-co-poly(MAA) hydrogels and pure components (psyllium, PEG, MAA, grafted system; Fig. 14). IPG's DSC showed an endothermic peak (55–100 °C) from bound water loss and exothermic degradation (~320 °C), aligning with Ahmad et al. (2020) on psyllium arabinoxylan. TGA revealed two IPG degradation stages: 10.11% loss at ~98.5 °C (initial), followed by major loss from decarboxylation, unsaturation, and polymer breakdown.

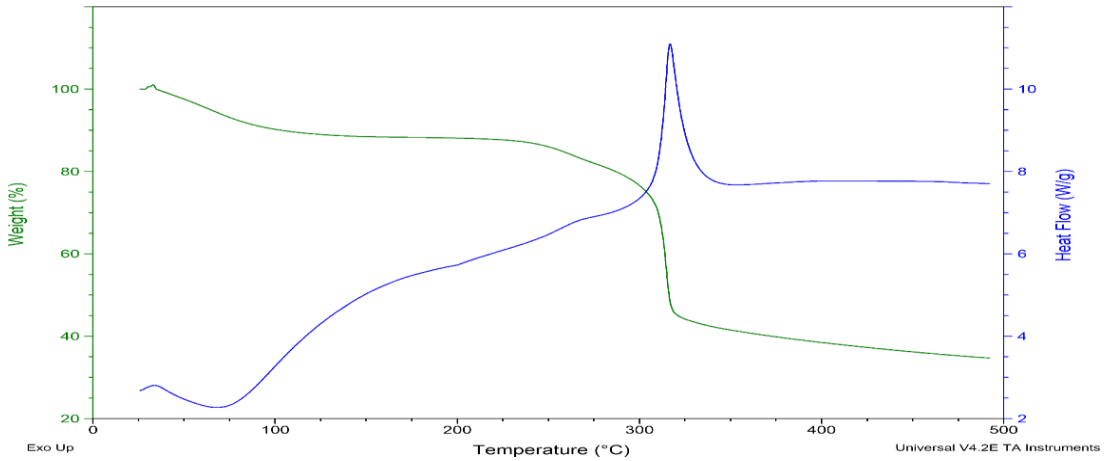

Figure 14. DSC and TGA thermograms of ispaghul psyllium gel

DSC spectrum of PEG exhibited a pronounced endothermic peak at 61.37°C that was connected with the melting of polymer. Another wide and clear feature was noticed at 428.25°C displaying the decomposition of PEG. TGA thermogram of PEG displayed its weight loss stages at progressively elevated temperatures. As evident from the spectrum, weight loss of 14.31% was identified at 400.14°C that raised rapidly and reached a maximum of 98.14% at 450.89°C. DSC/TGA spectrum of PEG is presented in figure 15.

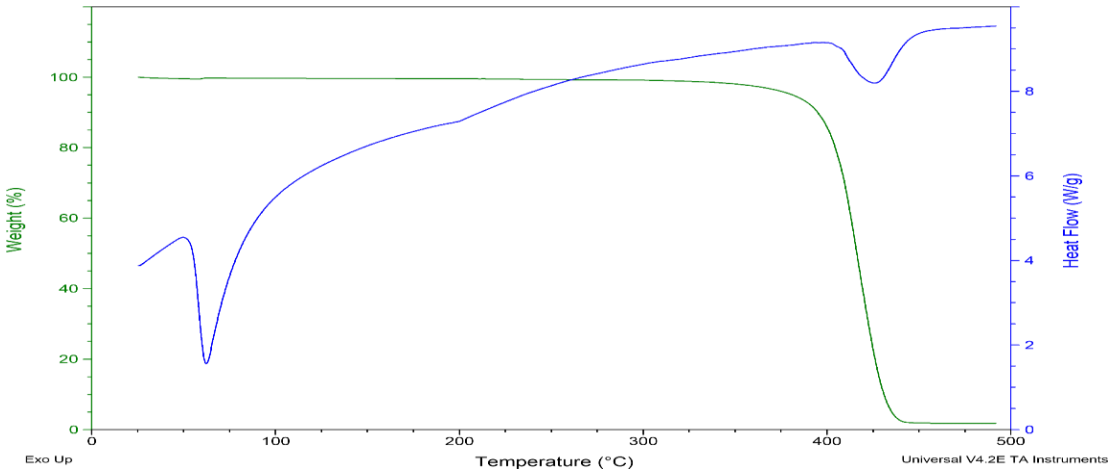

Figure 15. DSC and TGA thermograms of PEG 6000

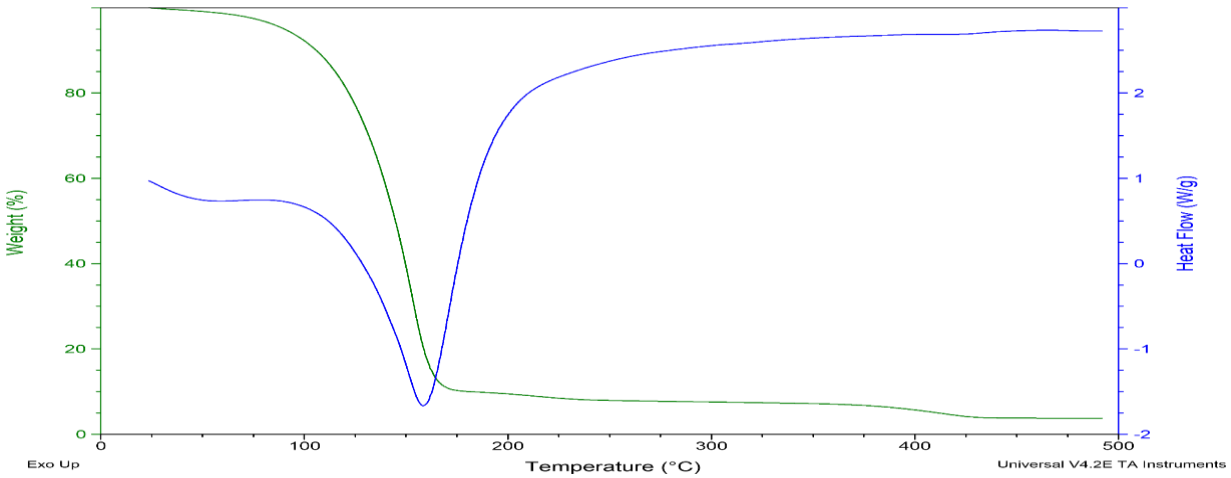

Figure 16. DSC and TGA thermogram of MAA

For methacrylic acid (MAA), a prominent endothermic band appeared at 165°C on its DSC thermogram. TGA spectrum of MAA demonstrated that the weight reduction phase started at 23.79°C exhibiting a mere 0.01% mass loss at this temperature which raised gradually at rising temperatures. At an elevated temperature of 150.50°C, weight loss was recorded to be 62.01% and increased further to 90% at 180.62°C of temperature.

For the unloaded psyllium/PEG-co-poly(MAA) hydrogel, DSC showed a broad transition (185.5–242.25 °C) from elevated PEG melting, minor network breakdown (~300.20 °C), and major degradation (460.45 °C)—indicating excellent thermal stability.

TGA confirmed this with weight loss at higher temperatures than pure IPG, PEG, or MAA, leaving 10.46% residue at 492.91 °C.

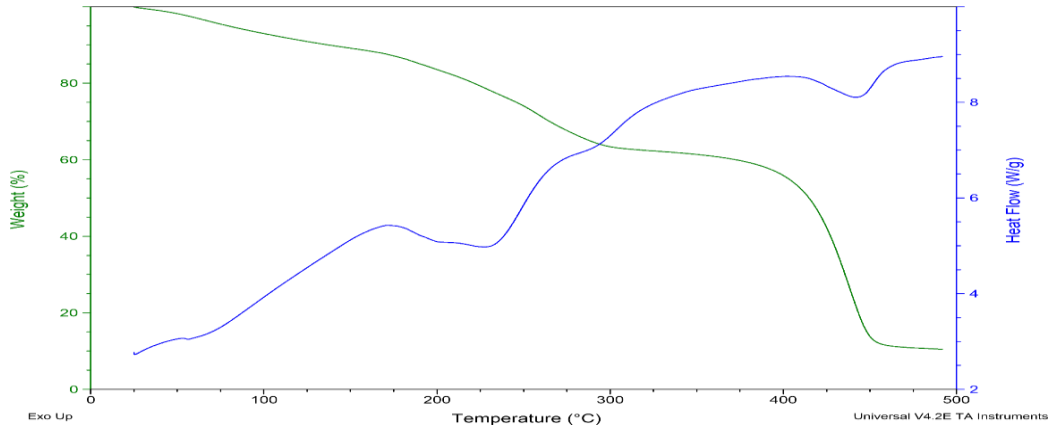

Figure 17. DSC and TGA thermogram of unloaded hydrogel

3.6 SEM analysis

SEM examined the psyllium/PEG-co-poly(MAA) hydrogel's surface morphology at 30×, 100×, 702×, and 1000× magnifications, revealing a dense, highly porous matrix with minor fractures and wavy features from chain overlap during drying (Fig 18).

These pores boost water uptake, swelling, drug loading, and controlled release—echoing Zahra et al. (2021) on PEG hydrogels for ivabradine delivery.

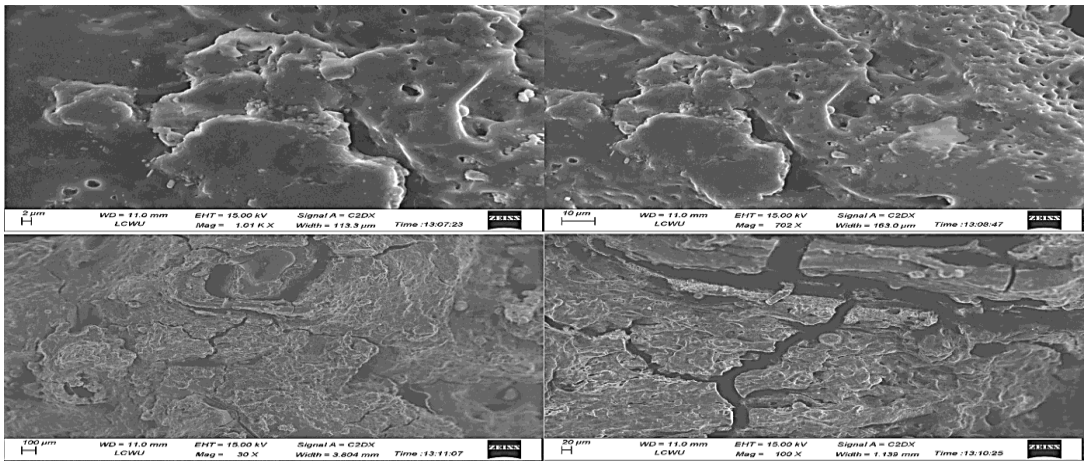

Figure 18. SEM photographs of psyllium/PEG-Co-Poly (MAA) hydrogel

3.7 Swelling experiments

The swelling capacity of the psyllium/PEG-based network was assessed by studies conducted in both acidic and alkaline environments (pH 1.2, 6 and 7.4 respectively). All network formulations showed a little swelling percentage at acidic pH (1.2) ranging from 6.85% to 12.96% as visible in figure 19. Nonetheless, significant swelling was seen at basic pH, demonstrating the hydrogels' pH-responsiveness. Selling capability was recorded as 40.20% to 67.57% for PsPM1-PsPM9 at pH 6, whereas it was noted as 67.31% to 97.01% at pH 7.4 as presented in figures 19, 20 and 21 respectively. Higher pH causes the monomer to produce additional carboxylate units, which repel polymeric chains and cause the system to gradually swell. A grafted system based on guar gum was created by Reddy et al. (2018), who discovered a comparable swelling capability at alkaline pH.

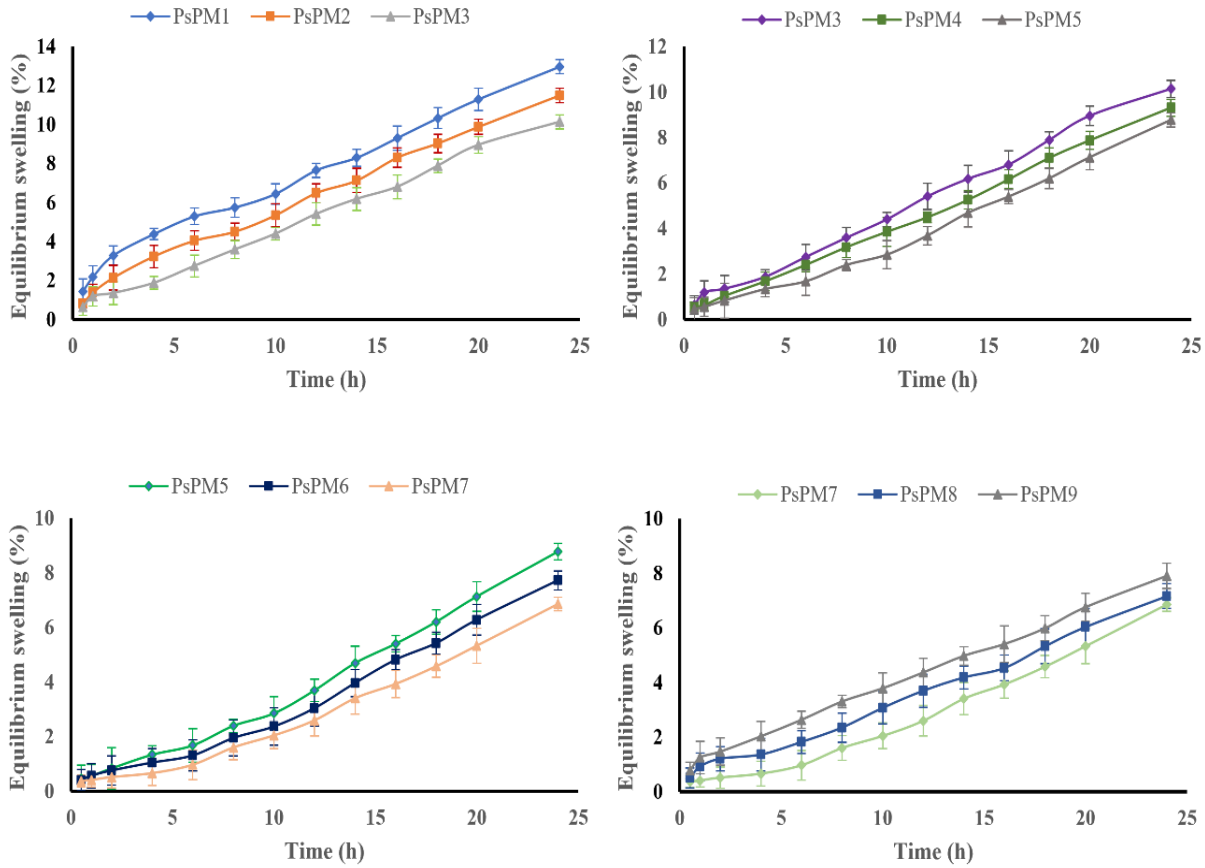

Figure 19. Swelling profile of PsPM1-PsPM9 at pH 1.2

Vol. 5 No. 1 (2026)

Pakistan Journal of Medical & Cardiological Review

https://pakjmcr.com/index.php/1/about

Online ISSN 3007-2387

Print ISSN 3007-2379

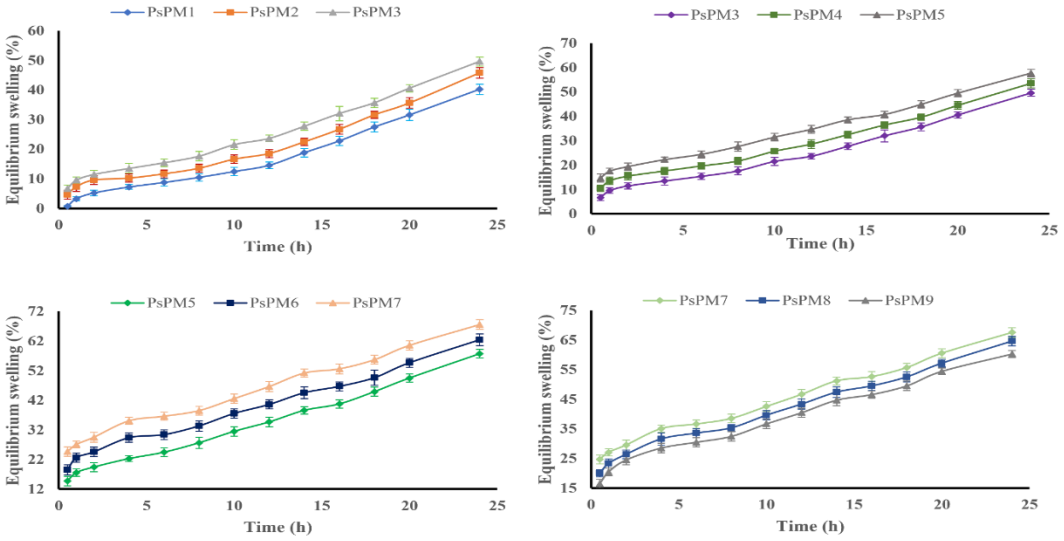

Figure 20. Swelling profile of PsPM1-PsPM9 at pH 6

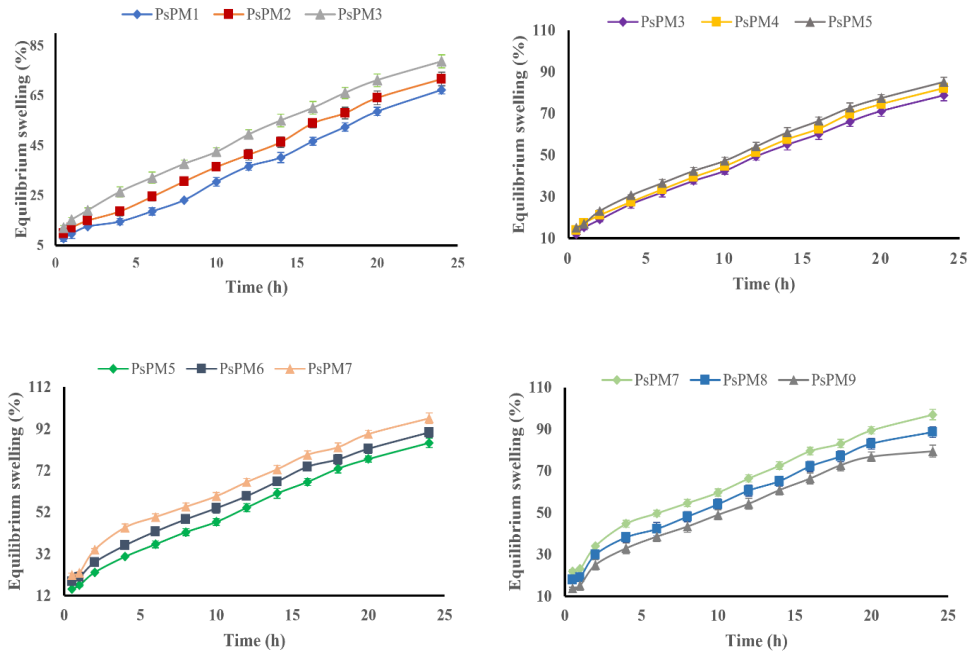

Figure 21. Swelling profile of PsPM1-PsPM9 at pH 7.4

We tested swelling (pH 7.4) across hydrogels by varying IPG, PEG, MAA, and MBA (Fig. 4.18). IPG increases (0.3–0.9 g; PsPM1–3) raised equilibrium swelling from 67.31% to 78.71%. PEG (0.15–0.6 g; PsPM3–5) boosted it to 85.26%, thanks to its hydrophilic -OH chains, making the network pH-responsive (Barkat et al., 2018). MAA (6–9 g; PsPM5–7) drove swelling to 97.01% via COOH dissociation and chain repulsion (Anirudhan & Mohan, 2018). Higher MBA (0.06–0.18 g; PsPM7–9) reduced it to 79.49% by tightening pores and stiffening the network.

3.8 *In-vitro* MBV release experiments

Dissolution tests (pH 1.2, 6.0, 7.4) showed minimal MBV release at pH 1.2 after 24 h, but steady increases at pH 7.4, driven by swelling (Fig 22).IPG (0.3–0.9 g; PsPM1–3) raised release to 65.32–74.21%; PEG (0.15–0.6 g; PsPM3–5) to 74.21–81.28% via hydrophilic -OH swelling.MAA (6–9 g; PsPM5–7) boosted it to 89.48% through COO^- repulsion (Asghar et al., 2018). Higher MBA (0.06–0.18 g; PsPM7–9) dropped release to 78.78% by densifying the network (Rafique et al., 2022).

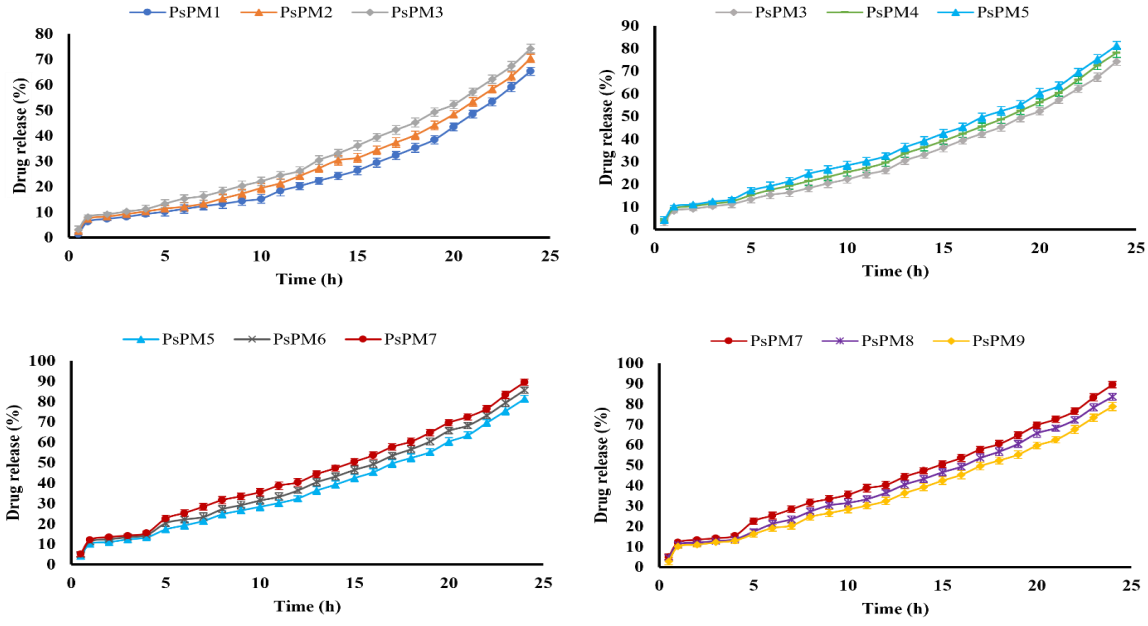

Figure 22. MBV release profile at pH 7.4

Kinetic modeling was performed on all tested networks' data (PsPM1-PsPM9) using Excel DD solver. Table 3 shows the findings of this modeling. The most suitable model and release process were identified by the regression coefficient (R^2) and exponent "n" values. The zero-order and Korsmeyer-Peppas models provided the best match for psyllium/PEG-co-(MAA) networks, representing R^2 values of 0.912-0.985 and 0.961-0.984, respectively. The hydrogel networks released MBV by a super case-II transport mechanism, exhibiting exponent n values of 0.929 to 1.518.

Table 2. Findings of kinetic models on MBV release data

Formulation Code	Zero Order	First Order	Higuchi	Hixson-Crowell	Korsmeyer-Peppas	
	R^2	R^2	R^2	R^2	R^2	n
PsPM1	0.912	0.853	0.687	0.872	0.961	1.518
PsPM2	0.942	0.881	0.727	0.902	0.971	1.361
PsPM3	0.961	0.899	0.761	0.921	0.975	1.239
PsPM4	0.967	0.907	0.784	0.929	0.974	1.154
PsPM5	0.975	0.918	0.808	0.940	0.976	1.076
PsPM6	0.979	0.924	0.829	0.947	0.978	1.012
PsPM7	0.980	0.936	0.858	0.957	0.981	0.929
PsPM8	0.985	0.932	0.831	0.954	0.984	1.015
PsPM9	0.980	0.929	0.817	0.949	0.980	1.053

Conclusion

The current research activities were conducted to produce an effective carrier network for regulated release of the antispasmodic agent Mebeverine HCl. A natural gum (polymer) obtained through Ispaghula psyllium seeds was combined with PEG 6000 (synthetic polymer) and cross-linked network was created using monomer (MAA) and cross-linking agent (MBA). Psyllium/PEG-co-MAA hydrogels were effectively produced and tested through the techniques of FTIR, TGA, DSC and

SEM. These tests have verified the excellent stability of hydrogels exhibiting the porous structure. Mebeverine loading % ranged from 61.08% to 85.98% for PsPM1-PsPM9. The swelling profile of network was outstanding at basic pH of 7.4 representing a maximum of 97.01% equilibrium swelling. The least swelling pattern was noticed at acidic pH (1.2). Likewise, network system presented the mebeverine release pattern extending up to 24 hrs. at 7.4 pH that ranged within 65.32%-89.48% for PsPM1-PsPM9. In conclusion, the findings of the research proved that psyllium/PEG-co-MAA system has tremendous potential in controlled.

References

Abu-Shawish, H. M., Ghalwa, N. A., Zaggout, F. R., Saadeh, S. M., Al-Dalou, A. R., & Abou Assi, A. A. (2010). Improved determination of tramadol hydrochloride in biological fluids and pharmaceutical preparations utilizing a modified carbon paste electrode. Biochemical Engineering Journal, 48(2), 237-245.

Ahmad, N., Tayyeb, D., Ali, I., K. Alruwaili, N., Ahmad, W., ur Rehman, A., ... & Iqbal, M. S. (2020). Development and characterization of hemicellulose-based films for antibacterial wound-dressing application. Polymers, 12(3), 548.

Almukhtar, J. G. J., & Karam, F. F. (2020). Preparation characterization and application of Chitosan nanoparticles as drug carrier. In Journal of Physics: Conference Series (Vol. 1664, No. 1, p. 012071). IOP Publishing.

Anirudhan, T. S., & Mohan, A. M. (2018). Novel pH sensitive dual drug loaded-gelatin methacrylate/methacrylic acid hydrogel for the controlled release of antibiotics. International Journal of Biological Macromolecules, 110, 167-178.

Asghar, S., Minhas, M. U., Ahmad, M., Khan, K. U., Sohail, M., & Khalid, I. (2018). Hydrophobic–hydrophilic cross-linked matrices for controlled release formulation of highly water-soluble drug venlafaxine: synthesis and evaluation studies. Advances in Polymer Technology, 37(8), 3146-3158.

Bahadur, S., Sahu, U. K., Sahu, D., Sahu, G., & Roy, A. (2017). Review on natural gums and mucilage and their application as excipient. Journal of applied pharmaceutical research, 5(4), 13-21.

Bajpai, A. K., & Giri, A. (2002). Swelling dynamics of a macromolecular hydrophilic network and evaluation of its potential for controlled release of agrochemicals. Reactive and Functional Polymers, 53(2-3), 125-141.

Barkat, K., Ahmad, M., Usman Minhas, M., Khalid, I., & Nasir, B. (2018). Development and characterization of pH-responsive polyethylene glycol-co-poly (methacrylic acid) polymeric network system for colon target delivery of oxaliplatin: Its acute oral toxicity study. Advances in Polymer Technology, 37(6), 1806-1822.

Batool, N., Mahmood, A., Sarfraz, R. M., Ijaz, H., Zafar, N., & Hussain, Z. (2021). Formulation and evaluation of interpenetrating polymeric network for controlled drug delivery. Drug Development and Industrial Pharmacy, 47(6), 931-946.

Bhardwaj, T. R., Kanwar, M., Lal, R., & Gupta, A. (2000). Natural gums and modified natural gums as sustained-release carriers. Drug development and industrial pharmacy, 26(10), 1025-1038.

Chawananorasest, K., Saengtongdee, P., & Kaemchantuek, P. (2016). Extraction and characterization of tamarind (Tamarind indica L.) seed polysaccharides (TSP) from three difference sources. Molecules, 21(6), 775.

Che, Y., Li, D., Liu, Y., Ma, Q., Tan, Y., Yue, Q., & Meng, F. (2016). Physically cross-linked pH-responsive chitosan-based hydrogels with enhanced mechanical performance for controlled drug delivery. RSC advances, 6(107), 106035-106045.

Chokboribal, J., Tachaboonyakiat, W., Sangvanich, P., Ruangpornvisuti, V., Jettanacheawchankit, S., & Thunyakitpisal, P. (2015). Deacetylation affects the physical properties and bioactivity of acemannan, an extracted polysaccharide from Aloe vera. Carbohydrate polymers, 133, 556-566.

Dickinson, R. G., Baker, P. V., Franklin, M. E., & Hooper, W. D. (1991). Facile hydrolysis of mebeverine in vitro and in vivo: negligible circulating concentrations of the drug after oral administration. Journal of pharmaceutical sciences, 80(10), 952-957.

Ganji, F., & VASHEGHANI, F. E. (2009). Hydrogels in controlled drug delivery systems. 63-88.

Gupta, V., Puri, R., Gupta, S., Jain, S., & Rao, G. K. (2010). Tamarind Kernel Gum: An Upcoming Natural Polysaccharide. Systematic Reviews in Pharmacy, 1(1).

Haensler, J., & Szoka Jr, F. C. (1993). Polyamidoamine cascade polymers mediate efficient transfection of cells in culture. Bioconjugate chemistry, 4(5), 372-379.

Hazer, O., Soykan, C., & Kartal, Ş. (2007). Synthesis and swelling behavior analysis of poly (acrylamidoxime-co-2-acrylamido-2-methylpropane sulfonic acid) hydrogels. Journal of Macromolecular Science, Part A: Pure and Applied Chemistry, 45(1), 45-51.

Hussain, H. R., Bashir, S., Mahmood, A., Sarfraz, R. M., Kanwal, M., Ahmad, N., ... & Nazir, I. (2022). Fenugreek seed mucilage grafted poly methacrylate pH-responsive hydrogel: A promising tool to enhance the oral bioavailability of methotrexate. International Journal of Biological Macromolecules, 202, 332-344.

Hussain, K., Aslam, Z., Ullah, S., & Shah, M. R. (2021). Synthesis of pH responsive, photocrosslinked gelatin-based hydrogel system for control release of ceftriaxone. Chemistry and Physics of Lipids, 238, 105101.

Jana, S., Sharma, R., Maiti, S., & Sen, K. K. (2016). Interpenetrating hydrogels of O-carboxymethyl Tamarind gum and alginate for monitoring delivery of acyclovir. International journal of biological macromolecules, 92, 1034-1039.

Ju, H. K., Kim, S. Y., & Lee, Y. M. (2001). pH/temperature-responsive behaviors of semi-IPN and comb-type graft hydrogels composed of alginate and poly (N-isopropylacrylamide). Polymer, 42(16), 6851-6857.

Karna, S., Chaturvedi, S., Agrawal, V., & Alim, M. (2015). Formulation approaches for sustained release dosage forms: a review. Asian J Pharm Clin Res, 8(5), 46-53.

Kiran, P., & Rao, P. S. (2016). Development and characterization of reconstituted hydrogel from Aloe vera (Aloe barbadensis Miller) powder. Journal of Food Measurement and Characterization, 10, 411-424.

Kosmala, J. D., Henthorn, D. B., & Brannon-Peppas, L. (2000). Preparation of interpenetrating networks of gelatin and dextran as degradable biomaterials. Biomaterials, 21(20), 2019-2023.

Kulkarni, R. V., & Sa, B. (2008). Novel pH-sensitive interpenetrating network hydrogel beads of carboxymethylcellulose-(polyacrylamide-grafted-alginate) for controlled release of ketoprofen: preparation and characterization. Current Drug Delivery, 5(4), 256-264.

Kumar, C. S., & Bhattacharya, S. (2008). Tamarind seed: properties, processing and utilization. Critical reviews in food science and nutrition, 48(1), 1-20.

Liang, Y., Zhao, X., Ma, P. X., Guo, B., Du, Y., & Han, X. (2019). pH-responsive injectable hydrogels with mucosal adhesiveness based on chitosan-grafted-dihydrocaffeic acid and oxidized pullulan for localized drug delivery. Journal of colloid and interface science, 536, 224-234.

Mahmood, A., Sharif, A., Muhammad, F., Sarfraz, R. M., Abrar, M. A., Qaisar, M. N., ... & Zaman, M. (2019). Development and in vitro evaluation of (β-cyclodextrin-g-methacrylic acid)/Na+-montmorillonite nanocomposite hydrogels for controlled delivery of lovastatin. International Journal of Nanomedicine, 5397-5413.

Malatani, R. T., Bilal, S., Mahmood, A., Sarfraz, R. M., Zafar, N., Ijaz, H., ... & Gad, H. A. (2023). Development of tofacitinib loaded pH-responsive chitosan/mucin-based hydrogel microparticles: in-vitro characterization and toxicological screening. Gels, 9(3), 187.

Mali, K. K., Dhawale, S. C., & Dias, R. J. (2017). Synthesis and characterization of hydrogel films of carboxymethyl tamarind gum using citric acid. International journal of biological macromolecules, 105, 463-470.

McConaughy, S. D., Stroud, P. A., Boudreaux, B., Hester, R. D., & McCormick, C. L. (2008). Structural characterization and solution properties of a galacturonate polysaccharide derived from Aloe vera capable of in situ gelation. Biomacromolecules, 9(2), 472-480.

Mudassir, J., & Ranjha, N. M. (2008). Dynamic and equilibrium swelling studies: crosslinked pH sensitive methyl methacrylate-co-itaconic acid (MMA-co-IA) hydrogels. Journal of Polymer Research, 15, 195-203.

Murali Mohan, Y., Sudhakar, K., Keshava Murthy, P. S., & Mohan Raju, K. (2006). Swelling properties of chemically crosslinked poly (acrylamide-co-maleic acid) hydrogels. International Journal of Polymeric Materials, 55(7), 513-536.

Muzzalupo, R., & Tavano, L. (2015). Niosomal drug delivery for transdermal targeting: recent advances. Research and reports in transdermal drug delivery, 23-33.

Naeem, A. (2017). Psyllium; an Effective Remedy for Common GI Problems. Available at SSRN 2960823.

Najafian, N., Aarabi, A., & Nezamzadeh-Ejhieh, A. (2022). Evaluation of physicomechanical properties of gluten-based film incorporated with Persian gum and Guar gum. International Journal of Biological Macromolecules, 223, 1257-1267.

Oryan, A., Alemzadeh, E., Mohammadi, A. A., & Moshiri, A. (2019). Healing potential of injectable Aloe vera hydrogel loaded by adipose-derived stem cell in skin tissue-engineering in a rat burn wound model. Cell and tissue research, 377, 215-227.

Pinheiro, M., Lucio, M., Lima, J. L., & Reis, S. (2011). Liposomes as drug delivery systems for the treatment of TB. Nanomedicine, 6(8), 1413-1428.

Rafique, N., Ahmad, M., Minhas, M. U., Badshah, S. F., Malik, N. S., & Khan, K. U. (2022). Designing gelatin-based swellable hydrogels system for controlled delivery of salbutamol sulphate: Characterization and toxicity evaluation. Polymer Bulletin, 79(7), 4535-4561.

Ranjha, N. M., Ayub, G., Naseem, S., & Ansari, M. T. (2010). Preparation and characterization of hybrid pH-sensitive hydrogels of chitosan-co-acrylic acid for controlled release of verapamil. Journal of materials science: Materials in Medicine, 21, 2805-2816.

Rao, P. S., Ghosh, T. P., & Krishna, S. (1946). Extraction and purification of tamarind seed polysaccharide. J Sci Ind Res, 4, 705.

Ravishankar, K., Venkatesan, M., Desingh, R. P., Mahalingam, A., Sadhasivam, B., Subramaniyam, R., & Dhamodharan, R. (2019). Biocompatible hydrogels of chitosan-alkali lignin for potential wound healing applications. Materials Science and Engineering: C, 102, 447-457.

Reddy, G. V., Reddy, N. S., Nagaraja, K., & Rao, K. K. (2018). Synthesis of pH responsive hydrogel matrices from guar gum and poly (acrylamide-co-acrylamidoglycolicacid) for anti-cancer drug delivery. Journal of Applied Pharmaceutical Science, 8(8), 084-091.

Sahraei, R., & Ghaemy, M. (2017). Synthesis of modified gum tragacanth/graphene oxide composite hydrogel for heavy metal ions removal and preparation of silver nanocomposite for antibacterial activity. Carbohydrate polymers, 157, 823-833.

Saraf, S. (2010). Applications of novel drug delivery system for herbal formulations. Fitoterapia, 81(7), 680-689.

Saraswathi, T. S., Mothilal, M., & Jaganathan, M. K. (2019). Niosomes as an emerging formulation tool for drug delivery-a review. IJAP, 11(2), 7-15.

Sharma, M., Mondal, D., Mukesh, C., & Prasad, K. (2014). Preparation of tamarind gum based soft ion gels having thixotropic properties. Carbohydrate polymers, 102, 467-471.

Shin, J., Braun, P. V., & Lee, W. (2010). Fast response photonic crystal pH sensor based on templated photo-polymerized hydrogel inverse opal. Sensors and Actuators B: Chemical, 150(1), 183-190.

Singh, A., Sharma, P. K., & Malviya, R. (2011). Release behavior of drugs from various natural gums and polymers. Polimery w medycynie, 41(4), 73-80.

Singh, R., Malviya, R., & Sharma, P. K. (2011). Extraction and characterization of tamarind seed polysaccharide as a pharmaceutical excipient. Pharmacognosy Journal, 3(20), 17-19.

Singh, B., Sharma, V., Kumar, R., & Mohan, M. (2022). Development of dietary fiber psyllium based hydrogel for use in drug delivery applications. Food Hydrocolloids for Health, 2, 100059.

Singh, S. K., Dhyani, A., & Juyal, D. (2017). Hydrogel: Preparation, characterization and applications. The Pharma Innovation, 6(6, Part A), 25.

Soppimath, K. S., Aminabhavi, T. M., Kulkarni, A. R., & Rudzinski, W. E. (2001). Biodegradable polymeric nanoparticles as drug delivery devices. Journal of controlled release, 70(1-2), 1-20.

Sudjaroen, Y., Haubner, R., Würtele, G., Hull, W. E., Erben, G., Spiegelhalder, B., ... & Owen, R. W. (2005). Isolation and structure elucidation of phenolic antioxidants from Tamarind (Tamarindus indica L.) seeds and pericarp. Food and chemical toxicology, 43(11), 1673-1682.

Suhail, M., Hsieh, Y. H., Shao, Y. F., Minhas, M. U., & Wu, P. C. (2021). Formulation and in-vitro characterization of pH-responsive semi-interpenetrating polymer network hydrogels for controlled release of ketorolac tromethamine. Gels, 7(4), 167.

Thorat, R. A. H. U. L., Patil, P. U. R. U. S. H. O. T. T. A. M., Aage, R. A. S. H. M. I., Puranik, P. R. A. S. H. A. N. T., & Salve, V. I. R. A. J. (2013). Formulation development and evaluation of venlafaxine HCl sustained release matrix tablet. Int. J. Pharma Sci Res, 5, 57-76.

Vahed, S. Z., Salehi, R., Davaran, S., & Sharifi, S. (2017). Liposome-based drug co-delivery systems in cancer cells. Materials Science and Engineering: C, 71, 1327-1341.

Zahra, Q., Minhas, M. U., Khan, S., Wu, P. C., Suhail, M., Iqbal, R., & Bashir, M. (2022). Fabrication of polyethylene glycol hydrogels with enhanced swelling; loading capacity and release kinetics. Polymer Bulletin, 79(7), 5389-5415.

D'souza, A. A., & Shegokar, R. (2016). Polyethylene glycol (PEG): a versatile polymer for pharmaceutical applications. Expert opinion on drug delivery, 13(9), 1257-1275.

Dey, R. K., Tiwary, G. S., Patnaik, T., & Jha, U. (2011). Controlled release of 5-aminosalicylic acid from a new pH responsive polymer derived from tamarind seed polysaccharide, acrylic acid, and polyamidoamine. Polymer bulletin, 66, 583-598.

Zhang, J., & Peppas, N. A. (2000). Synthesis and characterization of pH-and temperature-sensitive poly (methacrylic acid)/poly (N-isopropylacrylamide) interpenetrating polymeric networks. Macromolecules, 33(1), 102-107.

Raju, K. M., Raju, M. P., & Mohan, Y. M. (2002). Synthesis and water absorbency of crosslinked superabsorbent polymers. Journal of Applied Polymer Science, 85(8), 1795-1801.

Horwitz, B. J., & Fisher, R. S. (2001). The irritable bowel syndrome. New England journal of medicine, 344(24), 1846-1850.

Abdel-Hamid, S. M., Abdel-Hady, S. E., El-Shamy, A. H. A., & El-Dessouky, H. F. (2007). A novel formulation for mebeverine hydrochloride. Drug development and industrial pharmacy, 33(10), 1078-1089.

El Nabarawi, M. A., Teaima, M. H., Abd El-Monem, R. A., El Nabarawy, N. A., & Gaber, D. A. (2017). Formulation, release characteristics, and bioavailability study of gastroretentive floating matrix tablet and floating raft system of Mebeverine HCl. Drug design, development and therapy, 1081-1093.

Ahmed, E. M. (2015). Hydrogel: Preparation, characterization, and applications: A review. Journal of advanced research, 6(2), 105-121.

Ahmad, N., Ahmad, M. M., Alruwaili, N. K., Alrowaili, Z. A., Alomar, F. A., Akhtar, S., ... & Elkomy, M. H. (2021). Antibiotic-loaded psyllium husk hemicellulose and gelatin-based polymeric films for wound dressing application. Pharmaceutics, 13(2), 236.

Olad, A., Zebhi, H., Salari, D., Mirmohseni, A., & Reyhanitabar, A. (2018). A promising porous polymer-nanoclay hydrogel nanocomposite as water reservoir material: synthesis and kinetic study. Journal of Porous Materials, 25, 665-675.